

# Automatic well-testing model diagnosis and parameter estimation using artificial neural networks and design of experiments

Rouhollah Ahmadi<sup>1</sup> · Jamal Shahrabi<sup>2</sup> · Babak Aminshahidy<sup>1</sup>

Received: 20 July 2016 / Accepted: 24 October 2016 / Published online: 15 November 2016  
© The Author(s) 2016. This article is published with open access at Springerlink.com

**Abstract** The well-testing analysis is performed in two consecutive steps including identification of underlying reservoir models and estimation of model-related parameters. The non-uniqueness problem always brings about confusion in selecting the correct reservoir model using the conventional interpretation approaches. Many researchers have recommended artificial intelligence techniques to automate the well-testing analysis in recent years. The purpose of this article is to apply an artificial neural network (ANN) methodology to identify the well-testing interpretation model and estimate the model-related variables from the pressure derivative plots. Different types of ANNs including multi-layer perceptrons, probabilistic neural networks and generalized regression neural networks are used in this article. The best structure and parameters of each neural network is found via grid search and cross-validation techniques. The experimental design is also employed to select the most governing variables in designing well tests of different reservoir models. Seven real buildup tests are used to validate the proposed approach. The presented ANN-based approach shows promising results both in recognizing the reservoir models

and estimating the model-related parameters. The experimental design employed in this study guarantees the comprehensiveness of the training data sets generated for learning the proposed ANNs using fewer numbers of experiments compared to the previous studies.

**Keywords** Well-testing interpretation · Estimation · Classification · MLP · PNN · GRNN

## Introduction

The well-testing provides the required data for the qualitative and quantitative characterization of the reservoir. These data exhibit the real behavior of fluid flow throughout the reservoir as well as the near-wellbore region. So the parameters acquired by the well-testing data analysis are considered as one of the main data sources in establishing the reservoir management studies.

The interpretation of pressure transient data has two main objectives: (1) diagnosing the underlying conceptual reservoir model, and (2) estimating the model-related parameters. The well-testing analysis is an inverse solution to the reservoir model identification which is basically performed using the pressure derivative plots. The non-uniqueness problem, however, brings about confusion in selecting the correct reservoir model using the conventional approaches. The use of expert systems and artificial intelligence (AI) techniques has therefore been investigated by many authors in recent years to automate the process of recognizing the conceptual reservoir models and eliminate the existing problems in conventional analysis methods. Many approaches investigate the well-testing model identification using the AI techniques, whereas a few techniques have been developed to estimate the model-related parameters.

✉ Jamal Shahrabi  
jamalshahrabi@aut.ac.ir; jamalshahrabi@gmail.com  
Rouhollah Ahmadi  
rouhollah.ahmadi@aut.ac.ir; rouhollahahmadi@yahoo.com  
Babak Aminshahidy  
aminshahidy@aut.ac.ir; aminshahidy@gmail.com

<sup>1</sup> Department of Petroleum Engineering, Amirkabir University of Technology, Tehran Polytechnique, Tehran, Iran

<sup>2</sup> Department of Industrial Engineering and Management Systems, Amirkabir University of Technology, Tehran Polytechnique, Tehran, Iran

As the first attempt in automatic well-testing model identification using AI techniques, Allain and Horne (1990) employed syntactic pattern recognition and a rule-based approach to automatically recognize the conceptual reservoir models from the pressure derivative plots. To exhibit a significant improvement over the previous pattern recognition techniques, the application of ANNs for the automatic well-testing identification was founded by Al-Kaabi and Lee (1990). They used a back-propagation multi-layer perceptron (MLP) trained on representative examples of pressure derivative plots for a wide range of well test interpretation models in their work. The basic ANN approach of automatic well-testing diagnosis employed by Al-Kaabi and Lee (1990), which is the groundwork of many other studies in this regard, is briefly described in the following statements:

The pressure derivative curves are firstly sampled for a limited number of data points and normalized between 0 and 1 (or  $-1$  and 1) using different normalization techniques. The normalized derivative data points are then used as inputs to the neural networks. The output layer of ANN consists of the same number of nodes as the number of conceptual reservoir models considered in the problem. Each node in the output layer receives a score (activation level) between 0 and 1 representing the probability of occurring the corresponding reservoir model. The ANN examines the whole pressure derivative curve at the same time to identify the models causing the signals presented by the curve. The model corresponding to the output node with the largest activation level is considered as the most probable interpretation model. Figure 1 illustrates the general application of ANNs in determining the well-testing interpretation model using

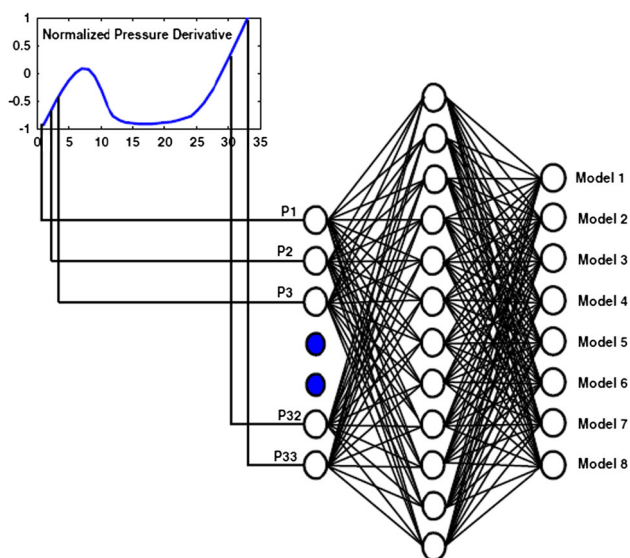


**Fig. 1** Application of ANN in the well-testing model identification with the pressure derivative plots as inputs and scores of different reservoir models as outputs of the network (Vaferi et al. 2011)

the pressure derivative curves. This figure is a typical example of the well-testing model diagnosis using ANNs. Although this figure shows 8 models at the output, the same ANN approach could be used for classifying any number of conceptual reservoir models. The improvements and modifications proposed by other researchers are briefly introduced in the following statements.

Al-Kaabi and Lee (1993) used modular neural networks, as combination of multiple smaller neural networks, to identify different model classes. A similar approach was proposed by Ershaghi et al. (1993) so as to use multiple neural networks with each network representing a single conceptual reservoir model due to disadvantages in using a single comprehensive neural network for covering all possible reservoir models. Juniardi and Ershaghi (1993) proposed a hybrid approach to augment the ANN models from an expert system with other information including independent field data and tables of frequency of occurrence of non-related models.

Kumoluyi et al. (1995) proposed to use higher-order neural networks (HONNs) instead of conventional MLP networks in identifying the well-testing interpretation model regarding both the scale and translation invariance of the well-testing models with respect to the field data. Athichanagorn and Horne (1995) presented an ANN approach combined with the sequential predictive probability (SPP) method to diagnose the correct reservoir models from the derivative plots. The SPP technique determines which candidate models predict the well response at the best provided that good initial estimates for the governing parameters of the candidate reservoir models are utilized. ANN was used to identify the characteristic components of the pressure derivative curves in terms of different flow regimes that might appear throughout the reservoir corresponding to each candidate reservoir model. Model parameters were then evaluated using the data in the identified range of the corresponding behavior using the conventional well-testing analysis techniques.

Sung et al. (1996) suggested the use of Hough transform (HT), as a unique technique for the extraction of basic shape and motion analysis in noisy images, combined with the back-propagation neural network to improve the well-testing model identification. An ANN approach was later proposed by Deng et al. (2000) to automate the process of type curve matching and move the tested curves to their sample positions. Unlike the previous approaches that used data point series as input vectors to train ANNs, the binary vectors of theory curves created by transferring the actual derivative curves into binary numbers were used as training samples to train ANN. The well-testing model parameters are also estimated during the type curve matching process. Aydinoglu et al. (2002) proposed an ANN approach to estimate different model parameters for the faulted

reservoirs. The network development begins with a simple architecture and a few input and output features and the level of complexity of the system are heuristically and gradually increased as more model parameters tend to be predicted by the network.

Jeirani and Mohebbi (2006) designed an MLP network to estimate the initial pressure, permeability and skin factor of oil reservoirs using the pressure build up test data. In fact, ANN was iteratively used to compute the bottom-hole shut-in pressure as a function of the Horner time, during the steps of estimating the permeability and the skin factor. Alajmi and Ertekin (2007) utilized an ANN approach to solve the problem of parameter estimation for double-porosity reservoir models from the pressure transient data using a similar procedure as employed by Aydinoglu et al. (2002). The complexity of ANN is increased step by step by removing one of the parameters from the input layer at each stage and adding it to the output layer to be included as one of the outputs of the network. Kharrat and Razavi (2008) employed multiple MLP networks of the same structure to identify multiple reservoir models from the pressure derivative data. All networks are trained using the whole set of training data for all the considered models. Application of ANNs in the well-testing model identification was also investigated by Vaferi et al. (2011). They attempted to use an MLP network with the optimum architecture to solve the well-testing diagnosis problem.

Regarding the previous studies on the application of ANNs in automating well-testing analysis, the following remarks are highlighted:

1. As ANNs provide great abilities in generalizing their understanding of the pattern recognition space they are taught to identify, they can identify patterns from incomplete, noisy and distorted data which is common to pressure transient data collected during the well tests.
2. Using ANNs, the needs for elaborate data preparation as employed in the rule-based approaches (including smoothing, segmenting, and symbolic transformation) and the definition of complex rules to identify the patterns are eliminated. Instead of using rules, an internal understanding of the pattern recognition space is automatically inspired in the form of weights that describe the strength of the connections between the network processing units.
3. Although some network parameters including the number of layers or hidden neurons were selected in a manner to achieve the best performance of classification or estimation, no organized and comprehensive framework was proposed by the previous authors for selection of the best architectures and parameters of ANNs.
4. The previous approaches used the analytically or numerically designed synthetic well-testing models to train the proposed neural networks. In addition, the number of training examples was determined using a predefined range of the governing parameters of the well-testing interpretation models. The governing parameters, however, are not selected based on a statistical criterion. No experimental designs were used for generating a statistically sufficient training data set for learning different ANNs.
5. The methods proposed previously for estimating different well-testing variables require a complex rule definition; the functional links defined in the input neurons of ANNs are determined subjectively, not based on a scientific benchmark.
6. Only two different types of ANNs including MLP and HONN, combined with other statistical techniques, were used in the well-testing interpretation in the previous studies. No attempts were made in applying other kinds of ANNs for diagnosing the underlying reservoir models and/or estimating the well-testing variables.

To alleviate the weaknesses and shortcomings of the previous studies listed above, this research proposes a more comprehensive methodology using different types of ANNs to effectively determine the conceptual reservoir models and estimate the model-related parameters from the pressure derivative plots. The best architecture and parameters of the proposed ANNs will be found using grid search (GS) and cross-validation (CV) techniques. The experimental design is also employed prior to training ANNs to find out the most influential parameters of the well-testing models and generate a sufficient number of training examples for training the ANN-based models.

## The proposed methodology

Well-testing model identification and parameter estimation using different types of ANNs during the pressure buildup tests are the main contributions of this article. Another contribution reinforced by this article includes the use of experimental design for selection of the most governing factors involved in constructing different well-testing models as well as building a proper training data set used for learning the classification/estimation models. The proposed procedure is described in the following steps:

1. Experimental Design

- 1.1 The set of all parameters used for building a well-testing design for each conceptual reservoir model should be considered. These parameters may be divided into different categories including well parameters, reservoir rock and fluid properties, reservoir geometry information and production data before running a pressure buildup test.
  - 1.2 To determine the most influential variables, a proper screening design of experiment (DOE) is performed on the selected uncertain parameters. DOE proposes the sufficient number of experiments and determines the levels of all factors during each experiment. The term “*experiment*” in the application of well-testing interpretation refers to a well-testing design generated by the analytical or numerical models. Each experiment involves a pressure derivative curve plotted for the corresponding well-testing design that would be used for further analysis.
  - 1.3 Since the pressure derivative curves are considered as the time series objects of relatively high order, they are undertaken by sampling and dimensionality reduction techniques before proceeding to the next steps.
  - 1.4 Multiple analysis of variance (MANOVA) is used to analyze the results of DOE to screen the most significant well-testing variables from the initial set of parameters as determined in Step 1.
  - 1.5 A different DOE technique (e.g., fractional factorial design) is once more utilized to construct a statistically sufficient training data set for learning the proposed classification/estimation models using the significant parameters in Step 4.
2. ANN Modeling
    - 2.1 Training data are preprocessed using the appropriate techniques including filtering, sampling, dimensionality reduction and normalization methods before proceeding to the proposed models. Different types of ANNs including MLPs, generalized regression neural networks (GRNNs) and probabilistic neural networks (PNNs) are used to identify the well-testing interpretation model and estimate the model-related parameters subsequently. The targets

defined in the well-testing analysis are considered as the only output neuron of the neural network models. The permeability ( $K$ ), skin factor ( $S$ ), dimensionless wellbore storage ( $C_D$ ), storativity ratio ( $\omega$ ) and inter-porosity flow coefficient ( $\lambda$ ) are the well-testing variables that will be estimated using the proposed ANN-based model in this article depending on the type of reservoir model. The structure and parameters of the proposed neural networks are best identified via GS and K-fold CV techniques.

### 3. Model Validation

- 3.1 Real field buildup tests are finally used to validate the trained models by comparing the network outputs with the results of conventional well-testing analysis.

A simple schematic diagram of the proposed methodology is presented in Fig. 2. The proposed approach is not exclusive to any specific types of reservoir models and could be applied to oil and gas/gas condensate reservoirs with a variety of well geometries and reservoir structures, provided that the model is trained again using the new training examples of the considered reservoir models.

### DOE application

As described in “[The proposed methodology](#)” section, the proposed approach employs the experimental design in two steps including the screening design (Step 1.4 of “[The proposed methodology](#)” section) and the fractional factorial design (Step 1.5 of “[The proposed methodology](#)” section). The flowchart of DOE applications in the well-testing analysis is illustrated in Fig. 3.

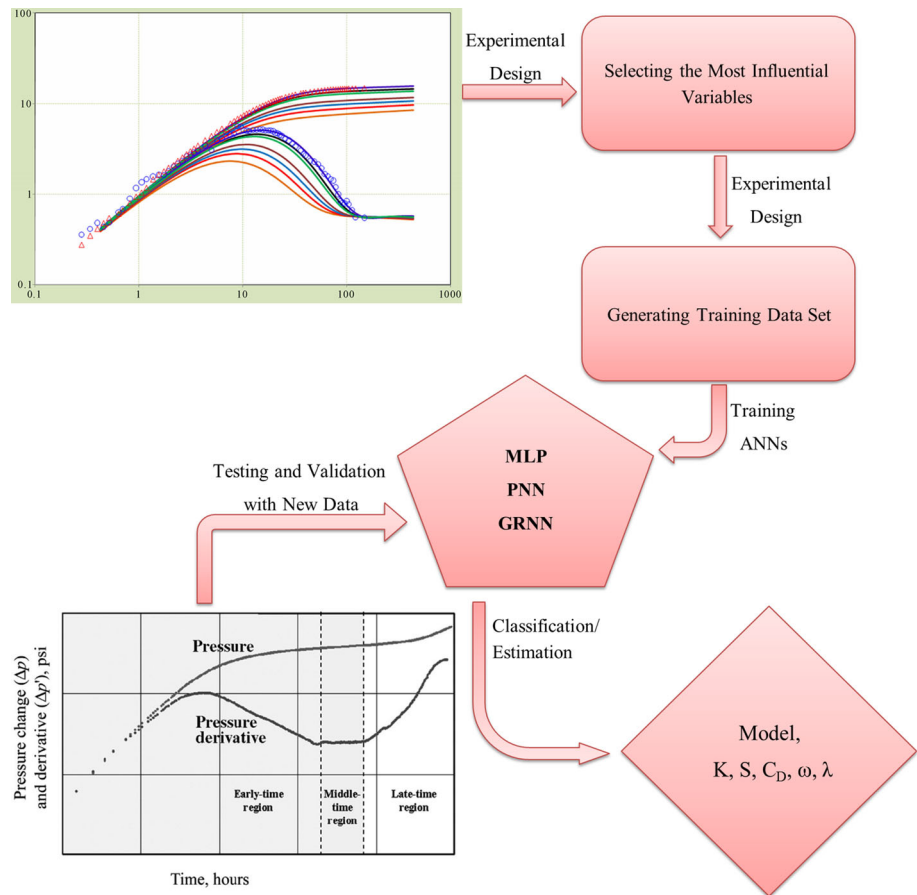
### Experimental design

Experimental design is the process of planning a study to meet the specified objectives. Planning an experiment properly is very important in order to ensure that the right type of data and a sufficient sample size and power are available to answer the research questions of interest as clearly and efficiently as possible. DOE is a systematic method to determine the relationship between the factors affecting a process and its output (Hinkelmann and Kempthorne 2007; Sundararajan 2015).

There are some outcomes beneficial to our application when the experimental design is utilized (Antony 2003; Montgomery 2002):

1. Recognition of input parameters and output results.

**Fig. 2** Schematic diagram of the proposed model for the well-testing interpretation and analysis using ANNs



2. Determination of the effects of input parameters on output results in a shorter time and lower cost.
3. Determination of the most influential factors.
4. Modeling and finding the relationship among input parameters and output results.
5. Better understanding of the process and system performance.

To use the experimental design effectively, the following guidelines as displayed in Fig. 4 are recommended (Jamshidnezhad 2015; Montgomery 2002):

1. *Recognition of uncertain parameters* There is a variety of uncertain variables (factors) in building a conceptual reservoir model as needed in a well-testing diagnosis problem. It helps to prepare a list of uncertain parameters that are to be studied by the experimental design.
2. *Choice of factors ranges and levels* In studying uncertain parameters, the reservoir engineer has to specify the range over which each factor varies. Wide range is recommended at the initial investigations (to screen the most influential factors). After selecting the most influential factors, the range of factor variations usually becomes narrower in the subsequent studies. In

3. *3 Selection of response variables* Selection of response variables should be done properly so that it provides useful information about the process. Typically in a well-testing problem, a number of points sampled on the pressure derivative plots or a useful transformation of them may be considered as the response variables.
4. *Selection of design method* There are several designs of experiments. In selecting the design, the objective of the study should be considered. The most appropriate designs are classical approaches like full factorial design, fractional factorial design and Plackett–Burman (PB) design (Antony 2003).

In full factorial designs, the experimental runs are performed at all combinations of factor levels. However, as the number of factors or factor levels in full factorial design increases, the number of realizations increases exponentially which requires more budget and time. If some higher-order interactions between primary factors (e.g., third-order



**Fig. 3** Different guidelines of experimental design (resource from Jamshidnezhad 2015; Montgomery 2002)

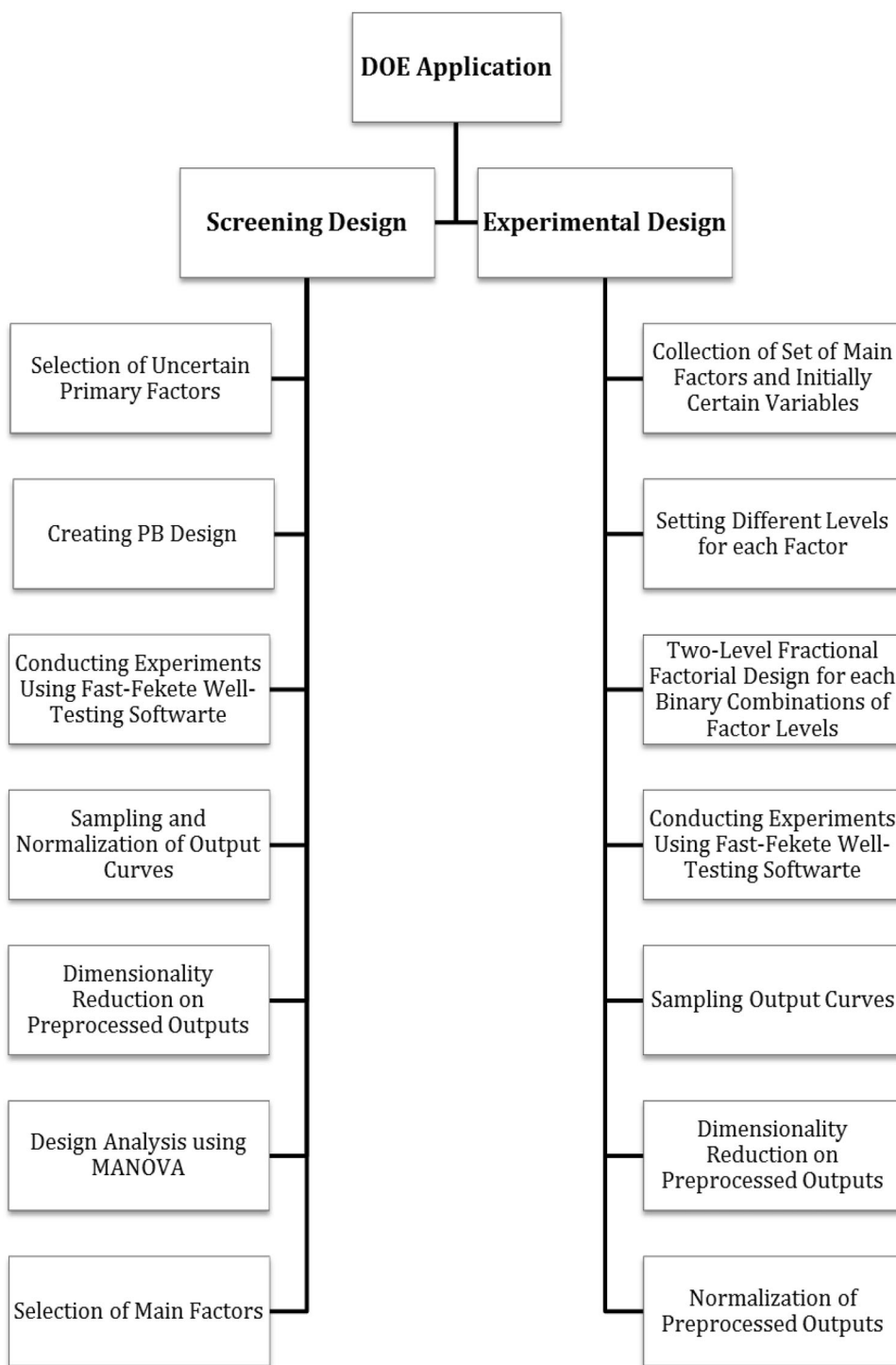


**Fig. 4** Flowchart of DOE applications in the well-testing analysis

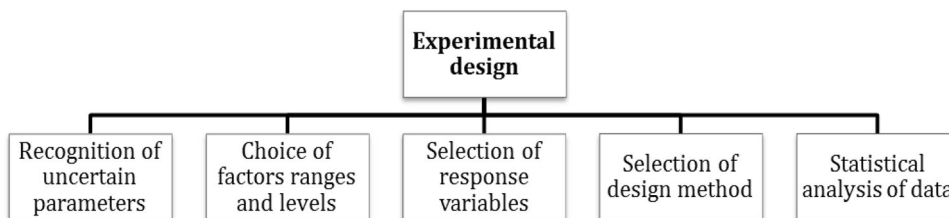


**Table 1** Application of different types of ANNs in the well-testing model diagnosis and parameter estimation

Type of ANN	MLP	GRNN	PNN
ANN task	Estimation (regression)	Estimation (regression)	Classification/prediction
ANN Output	Permeability Skin factor	Wellbore storage coefficient Storativity ratio	Inter-porosity flow coefficient Type of reservoir model

and higher) are assumed unimportant, then information on the main effects (primary factors) and two-order interactions can be obtained by running only a fraction of the full factorial experiment. This design is the most widely and commonly used type of design in the industry that is called fractional factorial design. PB design is one of the most commonly used of fractional factorial designs, as a standard two-level screening design (NIST Information Technology Laboratory 2012) that will be used as the screening strategy in this article.

5. *Statistical analysis of data:* In experimental design, for analyzing the data and obtaining the objective results and conclusions, statistical methods are employed. Analysis is usually done by a technique called analysis of variance (ANOVA) in which the differences between parameter means are analyzed.

ANOVAs evaluate the importance of one or more factors by comparing the means of response variables at different factor levels (Montgomery 2002; Nelson 1983). To run an ANOVA, there must be a continuous response variable and at least one categorical factor with two or more levels. The main output from ANOVA study is arranged in a table containing the sources of variation, their degrees of freedom, the total sum of squares, and the mean squares. The ANOVA table also includes the F-statistics and *p* values. These are employed to determine whether the predictors or factors are significantly related to the response. If the *p* value is less than a predefined alpha (usually  $\alpha = 0.05$ ), it can be concluded that at least one factor level mean is different.

When two or more response variables are considered, MANOVA should be used for analyzing the results. MANOVA is simply an ANOVA with several dependent variables (French et al. 2015).

**ANN application**

ANNs provide great capability and flexibility for estimation, prediction and classification purposes. As specified in Table 1, different types of ANNs including MLPs, GRNNs and PNNs are utilized for the well-testing model diagnosis and parameter estimation in this research.

The inputs, targets and architecture of ANNs proposed in this article are described in the following subsections.

*Inputs/targets of ANNs*

The ANNs require a representative and comprehensive training data set for an effective performance. A suitable training data set involving a wide variety of instances of the different well-testing models are generated using DOE as described previously in “The proposed methodology” section. The training inputs/targets data pairs that should be used for training different types of ANNs are described in the following subsections.

*Inputs* For any well-testing model created according to DOE techniques, several data points are sampled uniformly from the pressure derivative plots to extract a number of

**Table 2** Targets for training the proposed ANNs and estimating different well-testing parameters in the case of homogeneous and double-porosity systems (Equations are in field units from Bourdarot 1999; Lee 1982)

Well-testing parameter	ANN target	Equation for transforming the well-testing model parameter to the ANN target
Permeability ( <i>K</i> )	<i>m</i>	$m = \frac{162.6q_o\mu_oB_o}{Kh}$
Skin Factor ( <i>S<sub>d</sub></i> )	<i>p<sub>1h</sub></i>	$p_{1h} = m \cdot \left( \frac{S_d}{1.15} - \log\left(\frac{t_p+1}{t_p}\right) + \log\left(\frac{K}{\phi\mu_oC_1r_w^2}\right) - 3.23 \right) + p_{wf}(t_p)$
Dimensionless Wellbore Storage ( <i>C<sub>D</sub></i> )	<i>m<sub>C<sub>D</sub></sub></i>	$m_{C_D} = \frac{q_oB_o}{24C}; \quad C = \frac{C_D\phi C_1hr_w^2}{0.89}$
Storativity Ratio ( $\omega$ )	$\Delta p_\omega$	$\Delta p_\omega = m \cdot \log(\omega)$
Inter-porosity Flow Coefficient ( $\lambda$ )	$\lambda$	No transformation is needed

Where *q<sub>o</sub>*,  $\mu_o$  and *B<sub>o</sub>* are the oil production rate, oil viscosity and oil formation volume factor respectively; *h* is the formation thickness; *t<sub>p</sub>* means the production time before shutting-in the well;  $\phi$  stands for the formation porosity; *C<sub>1</sub>* is the total compressibility; *r<sub>w</sub>* shows the wellbore radius, and *p<sub>wf</sub>* implies the bottom-hole flowing pressure

data points for further analysis (selecting 30 data points is a common choice in this regard, as suggested by Al-Kaabi and Lee, 1990). Pre-processing techniques including dimensionality reduction and normalization are then applied on the sampled data. Principal component analysis (PCA) and singular value decomposition (SVD) are among the most common techniques of dimensionality reduction that could be employed for this purpose. The final training input data sets used for learning the classification/estimation models are created using the normalized data for all the classes considered.

**Targets** As previously declared, determination of the well-testing interpretation models and estimation of the model-related variables from the pressure derivative plots using different types of ANNs are the main objects of the present article. The first part could be regarded as a classification problem, whereas the second part is an estimation task.

For the classification purposes where the ANN tries to predict the correct label of conceptual reservoir models from the normalized pressure derivative data, the corresponding labels (i.e., reservoir classes) of the input data are used as the main targets for the trained networks.

To estimate the model parameters, on the other hand, a variable transformation is initially performed. During conventional well-testing interpretation, the reservoir models and their corresponding flow regimes are characterized on the pressure derivative plots. These flow regimes are described in the form of straight lines of different slopes or specific shapes on the well-testing diagnosis plots. The model parameters are then estimated using the slopes of different straight lines (Lee 1982). Therefore, in this article, rather than estimating the well-testing model parameters directly from the pressure derivative plots, the slopes of lines and some other related variables are considered as the main targets of the proposed ANN models. Such useful equations for the case of homogeneous and double-porosity reservoir models, as they are investigated later in “**Results and discussions**” section for testing the proposed ANN-based approach, are provided in Table 2. When predicted, the outputs of ANNs must be finally transformed back to the original well-testing parameters using the provided equations.

While MLP networks are suggested for estimating the permeability and skin factor values from the pressure derivative plots in this article, they are not recommended for estimating the values of wellbore storage coefficient, storativity ratio, and inter-porosity flow coefficient and for classifying the correct reservoir models using the pressure derivative data, due to relatively large MSE values of the MLP networks when modeling these parameters for the reservoir models considered in this article (“**Results and**

**discussions**” section). Other types of ANNs including GRNN and PNN are therefore investigated for modeling the variables the MLP networks are not capable of predicting. As will be discussed in “**PNNs/GRNNs**” section, PNN and GRNN have similar architectures, but there is a fundamental difference; probabilistic networks perform classification where the target variable is categorical, whereas GRNNs perform regression where the target variable is continuous.

GRNNs are recommended to estimate the values of wellbore storage coefficient and storativity ratio as they get continuous values when transformed to their corresponding variables according to the equations provided in Table 2. For the inter-porosity flow coefficient, however, no transformation is applied before passing the values to the neural network model; therefore, owing to the discrete nature of the values of the inter-porosity flow coefficient (where only a limited number of values is used for generating the training examples using the DOE technique), a classifier rather than a regressor would be used to predict their values. The PNN classifier is thus employed for predicting the values of inter-porosity flow coefficient from the pressure derivative plots. The classification and diagnosis of conceptual reservoir models is also performed using a PNN classifier.

#### *MLP networks*

MLPs are feed-forward ANN models mapping the sets of input data onto a set of appropriate outputs. An MLP consists of multiple layers of nodes in a directed graph, with each layer fully connected to the next one. Except for the input nodes, each node is a neuron (or processing element) with a nonlinear activation function. MLP utilizes a supervised learning technique called back-propagation for training the network (Rosenblatt 1961; Rumelhart et al. 1986). MLP is a modification of the standard linear perceptron and can distinguish data that are not linearly separable (Cybenko 1989).

A two-layer MLP network (including one input layer, one hidden layer and one output layer) with the optimum number of hidden neurons is capable of modeling the complex nonlinear functions (Haykin 1999). Therefore, two-layer MLP networks are proposed for estimating some of the well-testing model parameters in this research.

#### *PNNs/GRNNs*

A PNN, introduced by Specht (1990), is a feed-forward neural network, which was derived from the Bayesian network and a statistical algorithm called Kernel Fisher discriminant analysis. In a PNN, the operations are organized into a multilayered feed-forward network with four



layers including input layer, pattern layer, summation layer and output layer. The general architecture of PNNs is illustrated in Fig. 5.

There are several advantages using PNN instead of MLP for classification purposes; they are much faster and can be more accurate than MLP networks; and they are relatively insensitive to outliers and generate accurate predicted target probability scores.

GRNN, as proposed by Specht (1991), falls into the category of PNNs. Like other PNNs, it needs only a fraction of the training samples a back-propagation neural network would need. Using a PNN is especially advantageous due to its ability to converge to the underlying function of the data with only few training samples available. The additional knowledge needed to get the fit in a satisfying way is relatively small and can be done without any additional input by the user. This makes GRNN a very useful tool to perform predictions and comparisons of the system performance in practice. According to Bowden et al. (2005), GRNNs could be treated as supervised feed-forward ANNs with a fixed model architecture. The general structure of GRNNs is similar to that of PNNs as shown in Fig. 5.

The probability density function used in GRNN is the normal distribution function. Each training sample,  $X_j$ , is used as the mean of a normal distribution (Li et al. 2014):

$$Y(X, \sigma) = \frac{\sum_{j=1}^n Y_j \exp\left(-\frac{D_j^2}{2\sigma^2}\right)}{\sum_{j=1}^n \exp\left(-\frac{D_j^2}{2\sigma^2}\right)} \tag{1}$$

$$D_j^2 = (X - X_j)^T \cdot (X - X_j) \tag{2}$$

The distance,  $D_j$ , between the training sample  $X_j$  and the point of prediction  $X$ , is used as a measure of how well

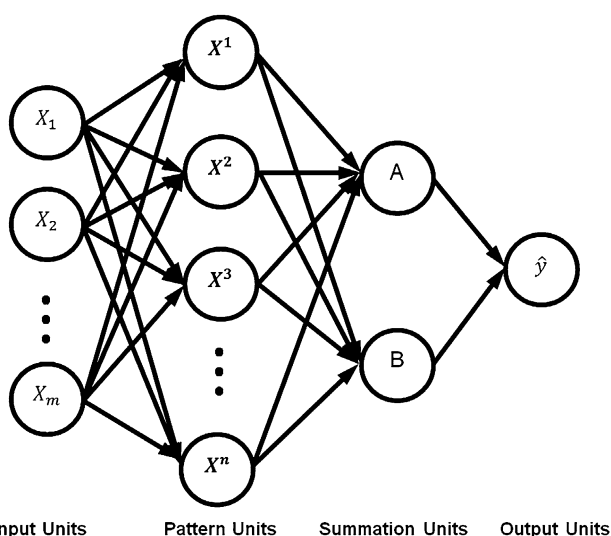


Fig. 5 General architecture of PNNs and GRNNs (based upon Gibbs et al. 2006)

each training sample can represent the position of prediction,  $X$ . Within Eqs. 1 and 2, the standard deviation or the smoothing parameter,  $\sigma$ , is the only unknown parameter that needs to be obtained through training (calibration). For a bigger smoothing parameter, the possible representation of the point of evaluation by the training sample is possible for a wider range of  $X$ .

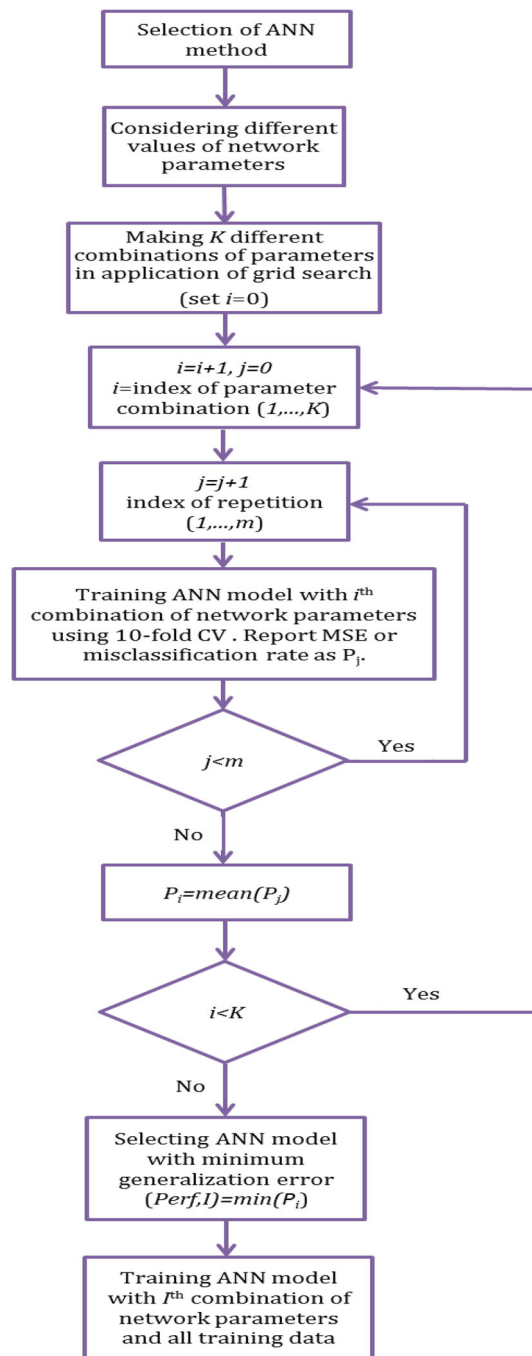


Fig. 6 General procedure of finding the best ANN parameters using GS and CV

As shown in Fig. 5, the structure of GRNN consists of four layers including input, pattern, summation and output units that are fully connected. According to Specht (1991), the input units are formed by the elements of the input vector  $X$ , feeding into each of the pattern units in the second layer. The sum of squared differences between an input vector  $X$  and the observed data  $X_j$ , is recorded in the pattern units as  $D_j^2$ . It then feeds into a nonlinear (e.g., exponential) activation function before passing into the summation units. The two parts,  $A$  and  $B$ , in the summation units correspond to the numerator and denominator in Eq. 1, respectively. The quotient of parts  $A$  and  $B$  is the predicted output by  $Y(X)$ .

The model architecture of GRNNs is fixed by the fact that the number of input nodes is determined by the number of inputs  $m$ , the number of pattern nodes depends on the size of the observed input data  $n$ , and the nodes in the summation units always consist of two parts including a denominator node and a numerator node.

#### Design of different types of ANNs

The following steps are considered in selecting the structure and parameters of the best ANN, as defined by the minimum generalization error, through application of GS

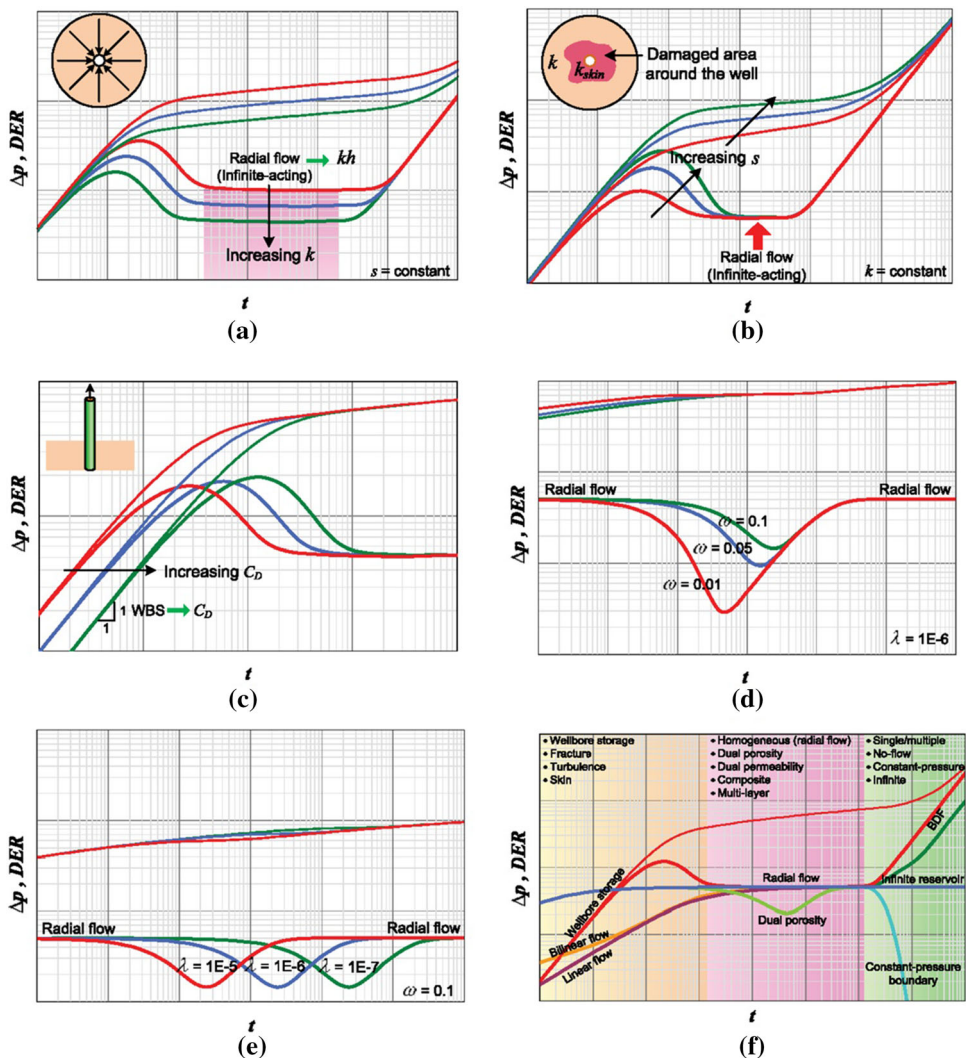
and CV techniques (as suggested by Ben-Hur and Weston (2015) in exploring the search space of hyper-parameters of the radial basis function kernels):

1. A range of values of the network parameters (including the number of hidden neurons, the network learning algorithm and the activation functions of different layers for MLPs, and the smoothing parameter for PNNs and GRNNs) is considered in learning multiple ANNs. Different combinations of the network parameters are used in an iterative manner through the GS technique for building the ANN models. Each network is trained using tenfold CV technique for an improved estimation of the generalization error of the network. To eliminate bias of error estimation, CVs are repeated multiple times and the estimated generalization errors are averaged over the repetitions. MSE values are considered as the performance criteria of MLPs and GRNNs, while the misclassification rate is used to measure the performance of PNN classifiers. Normalized pressure derivative data points are considered as inputs to the networks, while the well-testing variables according to the equations provided in Table 2 are used as the targets.
2. The network with the minimum generalization error is selected as the best ANN.

**Table 3** The list of all parameters involved in the well-testing design of VH/VDP models

Type of variable	Variable	Symbol	Type of reservoir model
Reservoir rock properties	Permeability	$K$	VH/VDP
	Net pay thickness	$h$	VH/VDP
	Skin factor	$S_d$	VH/VDP
	porosity	$\phi$	VH/VDP
	Storativity ratio	$\omega$	VDP
	Inter-porosity flow coefficient	$\lambda$	VDP
Wellbore properties	Dimensionless wellbore storage	$C_D$	VH/VDP
	Wellbore radius	$r_w$	VH/VDP
Reservoir geometry	Reservoir extent	$X_e (Y_e)$	VH/VDP
	Reservoir outer boundary	Boundary	VH/VDP
Production data	Production time	$t_p$	VH/VDP
	Production rate	$q_o$	VH/VDP
Reservoir fluid properties	Initial reservoir pressure	$P_i$	VH/VDP
	Water saturation	$S_w$	VH/VDP
	Reservoir temperature	$T_{res}$	VH/VDP
	API gravity	API	VH/VDP
	Oil formation volumetric factor	$B_o$	VH/VDP
	Oil viscosity	$\mu_o$	VH/VDP
	Total compressibility	$C_t$	VH/VDP
	Oil compressibility	$C_o$	VH/VDP
Solution gas oil ratio	$R_s$	VH/VDP	

**Fig. 7** Effect of different well-testing model parameters on shape of the pressure derivative plot; **a** permeability, **b** skin factor, **c** wellbore storage coefficient, **d** storativity ratio, **e** inter-porosity flow coefficient, and **f** outer boundary of reservoir (from IHS Energy Inc. 2015)



3. The best network is finally trained using all available training data.

The flowchart of selecting the best ANN parameters is also illustrated in Fig. 6.

### Results and discussions

To simply show the capabilities of the proposed approach in automating the well-testing analysis, two different conceptual reservoir models including vertical well in a homogeneous reservoir (VH) and vertical well in a double-porosity system (VDP) are investigated in this section. These cases are among the most common reservoir models occurred worldwide especially in the Iranian oil reservoirs. This article does not consider the well-testing analysis of more complex models using the presented approach that could be the subjects of future studies. Nevertheless, this approach

could be applied to more complex types of reservoir models including gas/gas condensate reservoir systems, partial penetration models, and horizontal/deviated wells from the pressure transient data, provided that the ANN-based model is reconstructed and re-trained using the new training examples of the considered reservoir models. To arrive at the automatic well-testing interpretation and analysis for the two reservoir models, different steps of the methodology proposed in “The proposed methodology” section are tracked in the following.

#### Screening design (first phase of DOE)

The parameters involved in creating both VH and VDP models are listed in Table 3. The VDP model involves a larger number of variables than the VH reservoir model when creating the well-testing designs. In other words, the VDP model is more comprehensive in the number of

**Table 4** The list of all variables involved in VDP model and their binary settings for PB design (The numbers in parentheses, where provided, are the corresponding values in SI units)

Variable	Setting of level +1	Setting of level -1	Field units (SI units)
$h$	100 (30.48)	1000 (304.79)	ft (m)
$\phi$	10	30	%
$r_w$	0.2 (0.06)	0.4 (0.12)	ft (m)
$X_e (Y_e)$	2000 (609.57)	6000 (1828.71)	ft (m)
$t_p$	50 (180,000)	120 (432,000)	hr (s)
$q_o$	500 (9.2E-4)	1500 (2.76E-3)	STBD (m <sup>3</sup> /s)
$P_i$	4000 (2.76E+7)	6000 (4.14E + 7)	psia (Pa)
$S_{wi}$	0	30	%
$T_{res}$	140 (60)	220 (104.44)	°F (°C)
API	25	40	degree
$B_o$	1 (1)	1.5 (1.5)	RBBL/STB (Rm <sup>3</sup> /Sm <sup>3</sup> )
$\mu_o$	0.5 (5E-4)	50 (0.05)	cp (Pa-s)
$C_t$	1e-6 (1.45E-10)	1e-5 (1.45E-9)	psi <sup>-1</sup> (Pa <sup>-1</sup> )
$C_o$	1e-6 (1.45E-10)	1e-5 (1.45E-9)	psi <sup>-1</sup> (Pa <sup>-1</sup> )
$R_s$	100 (17.81)	900 (178.11)	SCF/STB (Sm <sup>3</sup> /Sm <sup>3</sup> )

variables than the VH reservoir model. Therefore, the screening design will be directed only for the VDP model and the analyzed results are then applied to both VDP and VH models.

Some parameters listed in Table 3 play a clearly strong role in the well-testing diagnosis by affecting the shape of the pressure derivative curves. Therefore, these parameters are not included in the experimental design because of their certain effects. These variables include permeability, skin factor, wellbore storage coefficient, storativity ratio, inter-porosity flow coefficient and outer boundary of reservoir. The effect of these parameters on the pressure derivative plots is well illustrated in Fig. 7 and also described in the following statements (IHS Energy Inc. 2015):

1. As the permeability changes, the ordinate of the zero-slope straight line representative of the matrix flow moves vertically upward or downward (Fig. 7a).
2. Variation of the skin factor causes a noticeable change in the hump of the near wellbore phenomena (Fig. 7b).
3. A change in the wellbore storage coefficient shifts the unit-slope straight line at the start of pressure derivative curve horizontally along the time axis (Fig. 7c).
4. Changing the value of storativity ratio affects the dip depth of the fracture-matrix period for a double-porosity system (Fig. 7d).
5. Any changes in the inter-porosity flow coefficient causes a horizontal shift for the fracture-matrix dip in a fractured reservoir (Fig. 7e).
6. The type of reservoir outer boundary has a significant influence on the shape of the pressure derivative curve when the matrix radial flow has ended (Fig. 7f).

Therefore, among 21 parameters introduced in Table 3 for the VDP model, only 15 variables are considered in the experimental design. The experimental design in this study was performed using Minitab 17 software. In the first phase of DOE, the screening design is performed using PB design for selecting the most influential factors among 15 nominated variables.

As PB design is a two-level fractional factorial design, the list of all variables that should be investigated for the VDP model along with their binary settings are shown in Table 4. According to PB design, for the 15-factor well-testing diagnosis problem considered here, 49 experiments would be conducted among which 48 trials are performed at the two levels of each factor and 1 trial is conducted at their mean levels (Table 5). The rows and columns of Table 5 indicate the parameter index and the experiment number, respectively. The values -1, +1 and 0 correspond to the low, high and mean levels of each factor, respectively.

To create the corresponding well-testing models of pressure buildup tests according to the design table in Table 5, the Fast Fekete Well-Testing Software is employed. The models are synthesized analytically rather than numerically in this article. It should be noted that the created well-testing models are presumed to be single phase oil and the reservoir pressure is assumed to be above the bubble point pressure. The experiments are conducted according to the factor levels indicated in Table 5. The values of unaffected variables are kept constant during the experimentation phase according to Table 6. The outputs of the conducted experiments are the corresponding pressure derivative curves for the created pressure buildup

**Table 5** PB design table for 15 nominated well-testing parameters for VDP model; each P stands for a specific parameter according to the list of variables in Table 4

Experiment no.	P1	P2	P3	P4	P5	P6	P7	P8	P9	P10	P11	P12	P13	P14	P15
1	1	1	-1	1	-1	1	-1	-1	-1	1	1	-1	1	1	-1
2	1	1	-1	1	-1	1	-1	-1	1	1	1	1	-1	1	1
3	1	-1	1	-1	1	-1	-1	1	1	1	1	-1	1	1	1
4	-1	-1	1	1	-1	1	-1	1	-1	-1	-1	1	1	-1	1
5	-1	-1	-1	-1	1	1	-1	1	-1	1	-1	-1	-1	1	1
6	1	1	1	1	1	-1	-1	-1	-1	1	-1	-1	-1	-1	1
7	-1	-1	1	1	1	-1	1	-1	1	-1	-1	1	1	1	1
8	-1	1	-1	-1	-1	1	1	-1	1	1	-1	-1	1	-1	-1
9	1	1	-1	-1	-1	-1	1	-1	-1	-1	-1	1	1	-1	1
10	1	-1	-1	-1	-1	1	1	-1	1	-1	1	-1	-1	-1	1
11	-1	-1	-1	-1	-1	-1	-1	-1	-1	-1	-1	-1	-1	-1	-1
12	1	1	1	-1	-1	-1	-1	1	-1	-1	-1	-1	1	1	-1
13	-1	1	1	-1	1	1	-1	-1	1	-1	-1	1	1	1	-1
14	-1	1	-1	-1	-1	-1	1	1	-1	1	-1	1	-1	-1	-1
15	-1	1	-1	-1	1	1	1	1	-1	1	1	1	1	1	-1
16	1	1	1	1	-1	1	1	1	1	1	-1	-1	-1	-1	1
17	1	1	1	1	-1	-1	-1	-1	1	-1	-1	-1	-1	1	1
18	1	-1	-1	-1	-1	1	-1	-1	-1	-1	1	1	-1	1	-1
19	-1	1	1	1	-1	1	-1	1	-1	-1	1	1	1	1	-1
20	1	-1	-1	1	-1	-1	1	1	1	-1	1	-1	1	-1	-1
21	-1	-1	1	1	1	1	-1	1	1	1	1	1	-1	-1	-1
22	1	-1	-1	1	1	1	1	-1	1	1	1	1	1	-1	-1
23	-1	-1	-1	1	1	-1	1	-1	1	-1	-1	-1	1	1	-1
24	-1	1	1	-1	1	-1	1	-1	-1	-1	1	1	-1	1	1
25	1	1	-1	1	1	1	1	1	-1	-1	-1	-1	1	-1	-1
26	-1	1	-1	1	-1	-1	1	1	1	1	-1	1	1	1	1
27	1	1	-1	1	1	-1	-1	1	-1	-1	1	1	1	-1	1
28	-1	-1	-1	1	1	-1	1	1	-1	-1	1	-1	-1	1	1
29	1	1	1	-1	1	1	1	1	1	-1	-1	-1	-1	1	-1
30	-1	1	-1	-1	1	1	1	-1	1	-1	1	-1	-1	1	1
31	1	1	-1	-1	1	-1	-1	1	1	1	-1	1	-1	1	-1
32	1	-1	1	1	1	1	1	-1	-1	-1	-1	1	-1	-1	-1
33	-1	1	-1	1	-1	-1	-1	1	1	-1	1	1	-1	-1	1
34	-1	-1	1	1	-1	1	1	-1	-1	1	-1	-1	1	1	1
35	-1	-1	-1	-1	1	-1	-1	-1	-1	1	1	-1	1	-1	1
36	1	-1	-1	-1	1	1	-1	1	1	-1	-1	1	-1	-1	1
37	-1	-1	1	-1	-1	-1	-1	1	1	-1	1	-1	1	-1	-1
38	1	-1	-1	1	1	1	-1	1	-1	1	-1	-1	1	1	1
39	-1	1	1	1	1	1	-1	-1	-1	-1	1	-1	-1	-1	-1
40	-1	1	1	-1	-1	1	-1	-1	1	1	1	-1	1	-1	1
41	-1	-1	-1	1	-1	-1	-1	-1	1	1	-1	1	-1	1	-1
42	0	0	0	0	0	0	0	0	0	0	0	0	0	0	0
43	-1	1	1	1	1	-1	1	1	1	1	1	-1	-1	-1	-1
44	1	1	1	-1	1	-1	1	-1	-1	1	1	1	1	-1	1
45	1	-1	1	1	-1	-1	1	-1	-1	1	1	1	-1	1	-1
46	1	-1	1	-1	1	-1	-1	-1	1	1	-1	1	1	-1	-1
47	1	-1	1	-1	-1	-1	1	1	-1	1	1	-1	-1	1	-1
48	-1	-1	1	-1	-1	1	1	1	-1	1	-1	1	-1	-1	1
49	1	-1	1	-1	-1	1	1	1	1	-1	1	1	1	1	1



**Table 6** The values of unaffected well-testing variables during the experimentation phase (The numbers in parentheses, where provided, are the corresponding values in SI units)

Variable	$K$	$S_d$	$C_D$	$\omega$	$\lambda$	Reservoir outer boundary
Value	500 (4.95E–13)	0	2000	0.1	$1 \times 10^{-5}$	No flow
Field units (SI units)	md (m <sup>2</sup> )	Dimensionless				–

**Table 7** Results of conducting MANOVA study on PB design with 15 primary factors and reduced responses

Variable	$P_i$	$t_p$	$q_o$	$h$	$\phi$	$S_{wi}$	$C_t$	$r_w$	$X_e$	$T_{res}$	API	$\mu_o$	$B_o$	$C_o$	$R_s$
$p$ value	0.95	0.3	0	0	0	0.98	0	0	0	0.1	0.98	0	0	0.36	0.19

tests. The buildup tests are supposed to last enough so that the pressure derivative curves are entirely formed. Therefore, a long enough shut-in time was assumed for all the buildup tests.

Subsequent to the experimentation, the resulting pressure derivative curves are uniformly sampled at 30 data points. The extracted sets of points are then normalized using the min–max operator in Eq. 3:

$$X_{\text{new}} = \frac{X - \min(X)}{\max(X) - \min(X)} \quad (3)$$

where  $X$  and  $X_{\text{new}}$  are the sampled and normalized pressure derivative values, respectively.

The number of points sampled on the pressure derivative curves dictates the number of responses for PB design. To reduce further the number of responses, suitable dimensionality reduction techniques may be used. Singular value decomposition (SVD) is here employed for its major capabilities (Ientilucci 2003):

1. Transformation of the correlated variables into a set of uncorrelated ones to better reflect various relationships among the original data items.
2. Identifying and ordering the dimensions along which the data points exhibit the most variation.
3. Finding the best approximation of the original data using fewer numbers of dimensions.

What makes SVD practical for nonlinear problem applications is that the variation below a particular threshold could be simply ignored to massively reduce data assuring that the main relationships of interest have been preserved. In the present application, SVD is applied to the sampled pressure derivative data points. Dimensionality of the sampled data is then reduced from 30 to 4 dimensions regarding the cumulative relative variance provided by the selected dimensions reaching a predefined threshold (here 99.9% of the total variance). The remaining dimensions provide less than 0.1% of the total variance of data and

hence are ignored during further studies. MANOVA is then employed on the reduced data to analyze the screening design.

After performing MANOVA on PB design with reduced responses of the well-testing diagnosis problem, the  $p$  values for all the well-testing model parameters are shown in Table 7. As a result, only 7 variables among 15 nominated variables are considered as significant by comparing their  $p$  values against the chosen value of  $\alpha$  (equal to 0.05).

### Fractional factorial design (second phase of DOE)

The next steps during the well-testing interpretation and analysis including the well-testing designs, reservoir model diagnosis and evaluation of model parameters will be implemented using 13 variables (7 variables selected after the screening design plus 6 variables of less uncertainty discussed in “Screening design (first phase of DOE)” section). The well-testing diagnosis will be performed through the following steps:

1. The second phase of DOE is directed using a two-level fractional factorial design; the experiments are conducted using the Fast Fekete Well-Testing Software.
  - 1.1 All 13 variables previously selected are used in constructing the well-testing designs for the VDP model, while the storativity ratio and interporosity flow coefficient are excluded from studying the VH model as they are inherent to the naturally fractured reservoirs. The fractional factorial design for the VDP model consists of 129 runs for 13 variables at two levels including one center point at their mean levels. To better investigate the relationships among the model parameters (as the inputs) and the pressure derivative data points (as the model responses), the number of experiments could be increased

**Table 8** Different levels of the well-testing variables for the fractional factorial design (The numbers in parentheses, where provided, are the corresponding values in SI units)

Variable	1st level	2nd level	3rd level	4th level	Field units (SI units)
$K$	10 (9.87E-15)	100 (9.87E-14)	500 (4.93E-13)	1200 (1.18E-12)	md (m <sup>2</sup> )
$h$	20 (6.10)	200 (60.96)	1000 (304.79)	1800 (548.61)	ft (m)
$S_d$	5–	0	5	20	Dimensionless
$C_D$	100	1000	5000	10,000	Dimensionless
$\omega$	0.001	0.05	0.1	0.3	Dimensionless
$\lambda$	$1 \times 10^{-8}$	$1 \times 10^{-6}$	$1 \times 10^{-5}$	$1 \times 10^{-4}$	Dimensionless
$\phi$	5	15	20	30	%
$C_t$	$1 \times 10^{-6}$ (1.45E-10)	$5 \times 10^{-6}$ (7.25E-10)	$1 \times 10^{-5}$ (1.45E-9)	$5 \times 10^{-5}$ (7.25E-9)	psi <sup>-1</sup> (Pa <sup>-1</sup> )
$r_w$	0.25 (7.6E-2)	0.3 (9.1E-2)	0.35 (0.11)	0.4 (0.12)	ft (m)
$X_c$	1500 (457.18)	3000 (914.36)	4000 (1219.14)	5000 (1523.93)	ft (m)
$q_o$	500 (9.2E-4)	1500 (2.76E-3)	2500 (4.60E-3)	4000 (7.36E-3)	STBD (m <sup>3</sup> /s)
$\mu_o$	0.5 (5E-4)	5 (5E-3)	15 (0.015)	40 (0.04)	cp (Pa-s)
$B_o$	1	1.1	1.2	1.3	RBBL/STB (Rm <sup>3</sup> /Sm <sup>3</sup> )

**Table 9** The number of training examples used for building different types of ANNs

ANN	Target	Number of training examples
MLP1	Permeability	1164
MLP2	Skin factor	1164
GRNN1	Wellbore storage Coefficient	1164
GRNN2	Storativity ratio	774
PNN1	Inter-porosity flow coefficient	774
PNN2	Type of reservoir model	1164

and more number of factor levels may be examined. To consider wider ranges of values of the well-testing variables common to the Iranian oil reservoirs, four different levels are defined for each input variable according to the values provided in Table 8. The fractional factorial design is then accomplished for any binary combinations of the factor levels. So the number of repetitions of two-level DOEs (each containing 129 experiments) equals  $\binom{4}{2} = 6$  when taking all the factor levels into account. Therefore, the total number of experiments considered for the VDP model is equal to  $6 \times 129 = 774$  experiments.

- To conduct a two-level fractional factorial design for the VH model with 11 parameters, a design

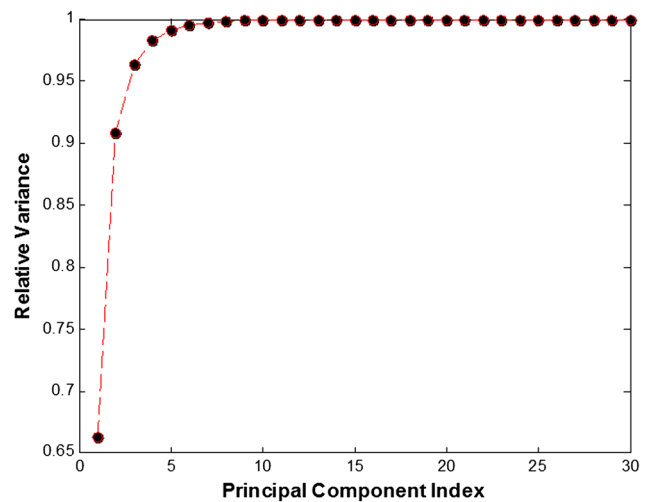


**Fig. 8** The scree plot of PCA results; the first 8 components comprise 99.9% of the total energy of data

table containing 65 experiments is created. Similarly, when defining four different levels for the selected factors according to Table 8, a number of  $6 \times 65 = 390$  experiments are totally considered for the VH model.

2. At the end of the second phase of DOE, the training data sets involving a wide variety of well-testing samples both for VDP and VH reservoir models are generated. The number of training examples used for building different types of ANNs is shown in Table 9.
  - 2.1 For any well-testing model created according to the DOE tables, the pressure derivative plots are sampled uniformly to extract 30 data points for further analysis.
  - 2.2 Principal component analysis (PCA) is then applied on the sampled data for additional dimensionality reduction. Similar to the procedure for the SVD technique, the appropriate number of components could be selected using a predefined threshold, regarding the relative variance (power) the principal components provide. Using the scree plot, the relative variance of the components is plotted against the index of the components in a descending order. Regarding the scree plot in Fig. 8, the cumulative variance of the principal components approaches a threshold of 0.999 using the first 8 components. The other components are disregarded due to negligible variances shared by them on the total power of the data. The number of inputs to each ANN is therefore 8, equal to the number of principal components retrieved. Each ANN has also 1 neuron in its output layer to predict the requested parameter based on the equations in Table 2.
  - 2.3 The reduced data are then normalized using the min–max operator (Eq. 3) to lie between 0 and 1. The final training data sets used for learning the classification/estimation models are created using the normalized data for the VDP and VH classes.

## ANN application

The ANN models are now constructed using the training data sets generated with the help of DOE techniques in “Fractional factorial design (second phase of DOE)” section. MLPs, PNNs and GRNNs are employed for the well-testing model diagnosis and the model-related parameter estimation. The architectures of the networks are determined based on the methodologies described in “design of different types of ANNs” section.

### MLP

MLP networks are used to estimate the values of permeability and skin factor from the normalized and reduced pressure derivative data points. Multiple networks with different parameters and structures are created and compared in the framework of GS and CV techniques. The number of hidden neurons, the network learning algorithm and the activation functions of different layers are varied based on Table 10. The mean squared error (MSE) is commonly used as the performance criterion of the neural networks when they are used for prediction or regression tasks. So, the MLP network with the minimum generalization MSE is selected as the best MLP. The minimum MSE values of different MLP networks as well as the corresponding number of hidden neurons are shown in Table 11. As observed, the minimum error is obtained for the hyperbolic tangent sigmoid algorithm and the Bayesian regulation back-propagation function using 17 neurons in the hidden layer. The best set of network parameters is employed for building two individual MLP networks for estimating the transformed values of the permeability and the skin factor. The regression plots of both training and test data is represented in Fig. 9a through 9d for the two MLP networks considered. Figure 10a, b illustrate the plots of target values versus the MLP outputs of the permeability and skin factor transformed values, respectively. The circle markers on the plots indicate the target values, while the network outputs are shown by the stars. It should be noted that the permeability and skin factor values are estimated for both VH and VDP models, covering all 1164 training data, as indicated on the x-axes of the plots. There are good consistencies between the targets and the networks outputs for both parameters, as observed on the plots.

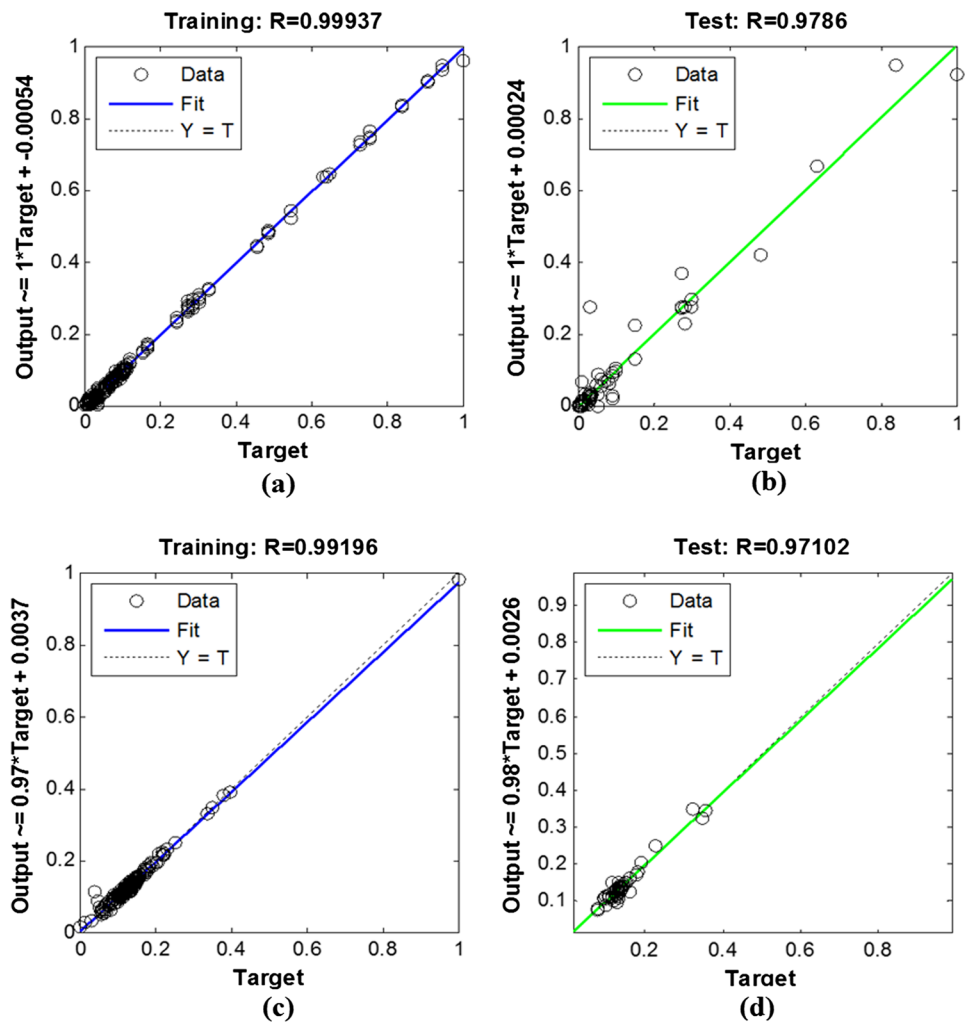
**Table 10** Different network parameters used in studying MLP networks

Number of hidden Neurons	Learning algorithm	Activation function
5 to 22	Levenberg–Marquardt backpropagation	Hyperbolic tangent sigmoid
	Bayesian regulation backpropagation	Log-sigmoid
	Scaled conjugate gradient backpropagation	Linear

**Table 11** Minimum MSE values and optimum number of hidden neurons used for selecting the best MLP networks in order to estimate the permeability and skin factor

Learning algorithm	Activation function	Minimum MSE	Number of hidden neurons
Hyperbolic tangent sigmoid	Levenberg–Marquardt backpropagation	0.00067	10
	Scaled conjugate gradient backpropagation	0.0091	22
	Bayesian regulation backpropagation	0.00041	17
Log-sigmoid	Levenberg–Marquardt backpropagation	0.19529	18
	Scaled conjugate gradient backpropagation	0.19589	10
	Bayesian regulation backpropagation	0.19589	7
Linear	Levenberg–Marquardt Backpropagation	0.0053	22
	Scaled conjugate gradient backpropagation	0.0053	5
	Bayesian regulation backpropagation	0.0053	7

**Fig. 9** The regression plots of MLP outputs versus targets for **a** training data of permeability, **b** test data of permeability, **c** training data of skin factor and **d** test data of skin factor



*PNNs/GRNNs*

PNNs are used to predict the underlying reservoir model and the discrete value of the inter-porosity flow coefficient

(if needed), while GRNNs are employed to estimate the values of dimensionless wellbore storage and storativity ratio (if required). Various networks with different smoothing parameters (from 0.01 to 0.5) are created and

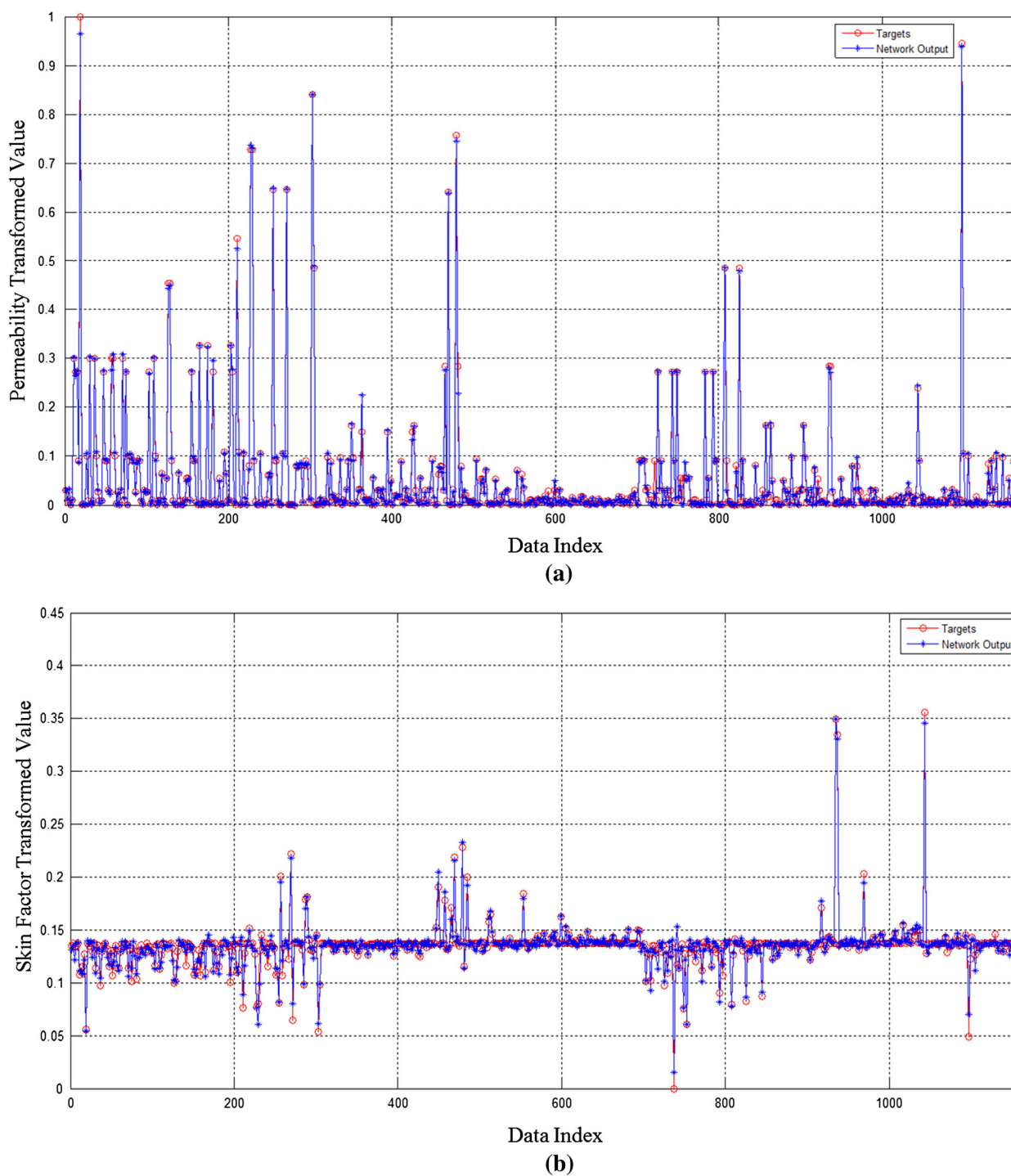


**Fig. 10** Plots of targets versus MLP outputs of **a** permeability transformed values, and **b** skin factor transformed values

compared through GS and CV techniques. The performance of different GRNNs versus the values of smoothing parameters is plotted and depicted in Fig. 11a, b for estimating the wellbore storage coefficient and the storativity ratio, respectively. The same plots are demonstrated in Fig. 11c, d for PNN classifiers used for modeling the interporosity flow coefficient and the well-testing reservoir

model, respectively. The smoothing parameter that yields the best performance of GRNNs/PNNs (corresponding to the minimum values of MSE and misclassification rate, respectively) is selected as the best smoothing parameter and will be used for further studies (Table 12).

The regression plots of both GRNNs used for estimating the wellbore storage coefficient and storativity ratio



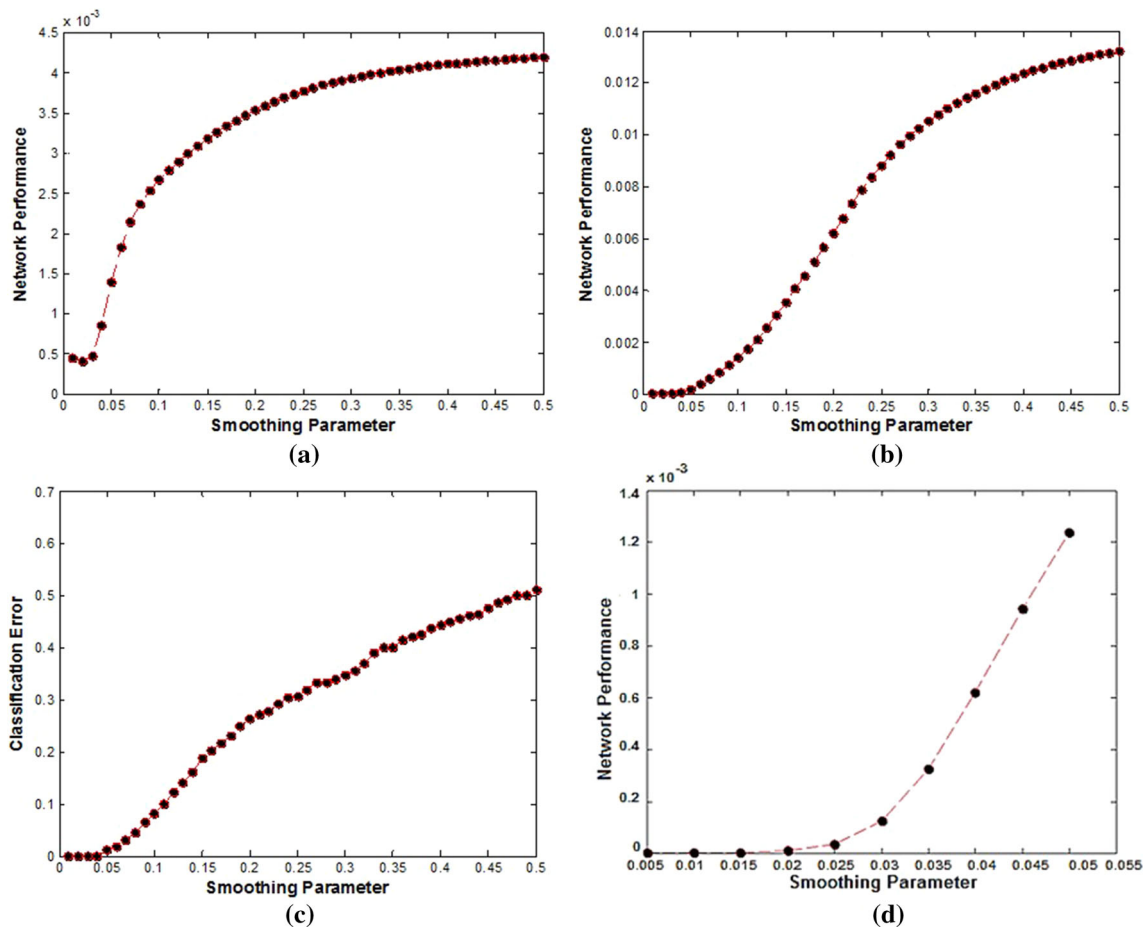


**Fig. 11** The performance plots of GRNNs and PNNs illustrating the network performance for different smoothing parameters used in constructing the neural networks, **a** GRNN for estimating the

wellbore storage coefficient, **b** GRNN for estimating the storativity ratio, **c** PNN for predicting the inter-porosity flow coefficient, and **d** PNN for classifying the well-testing reservoir model

**Table 12** The best values of smoothing parameters used in developing GRNNs and PNNs for modeling different variables

Variable	Wellbore storage coefficient	Storativity ratio	Inter-porosity flow coefficient	Well-testing reservoir model
Best smoothing parameter	0.02	0.01	0.01	0.01
Type of ANN	GRNN		PNN	

(trained using the best smoothing parameter and all available training data) are shown for the whole set of training and test data in Fig. 12a, b, respectively.

In addition, the targets versus the PNN outputs of the inter-porosity flow coefficient transformed values and the type of reservoir model are displayed in Fig. 13a, b, respectively. Figure 14a, b also exhibit the targets versus the GRNN outputs of the wellbore storage coefficient and storativity ratio transformed values, respectively. The circle markers on the plots indicate the target values, while

the network outputs are illustrated by the stars. As the x-axes of the plots show, the storativity ratio and inter-porosity flow coefficient values are estimated just for the VDP model with only 774 training examples, while other parameters of study are obtained for both VH and VDP models, covering all 1164 training data. According to the plots, there is a good agreement between the targets and the networks outputs for different parameters.

Finding the best structures and parameters of different MLPs, GRNNs and PNNs, the best performance of each

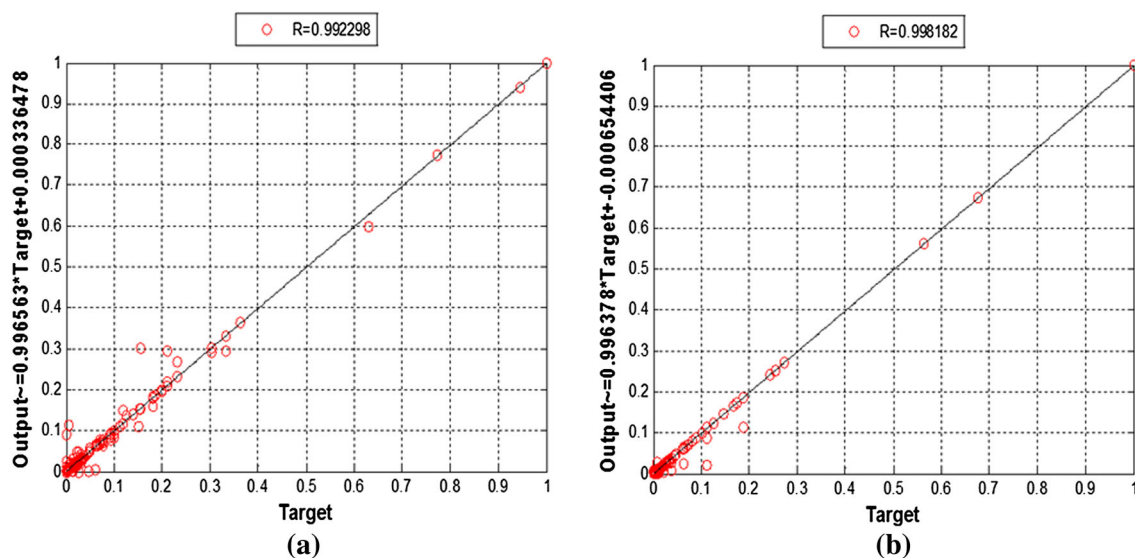


**Fig. 12** The regression plots of GRNN outputs versus targets for the whole set of training and test data for **a** wellbore storage coefficient, and **b** storativity ratio

neural network engaged for the estimation or classification purposes is illustrated in Table 13.

### Validation of trained models

To validate the proposed ANN-based models for the well-testing interpretation and analysis in this article, several case studies are tested here. These cases include seven real field buildup tests including three VDP and four VH reservoir models under different reservoir rock and fluid conditions producing at different oil rates.

In each case, the pressure derivative plot is firstly created from the pressure transient data. After proper manipulations and required preprocessing including sampling, dimensionality reduction and normalization (similar to the works described in “fractional factorial design (second phase of DOE)” section), the preprocessed derivative data points are fed as inputs into the neural network models including MLPs, PNNs and GRNNs. The network outputs are finally post-processed using the equations in Table 2 to determine the underlying reservoir model and estimate the model-related properties.

Some parameters including permeability, skin factor and wellbore storage coefficient are estimated for all the cases independent of the type of reservoir model. The well-testing model is then identified by the PNN classifier. The storativity ratio and the inter-porosity flow coefficient would be evaluated if the underlying reservoir model is classified as the double-porosity type. The seven test cases have also been analyzed using the conventional analysis techniques and the well-testing

model parameters have been estimated in this way. The validation results using the proposed model for the seven test cases in comparison with the conventional estimations are summarized in Table 14.

The relative errors of estimations using the proposed ANN-based model compared to the conventional analysis results are shown in Table 15.

As shown in Table 14, the proposed approach has correctly predicted the types of reservoir model for all the seven test cases. This confirms the presented model as a reliable (binary) classifier for determining the well-testing interpretation models using the pressure derivative plots. The model-related variables have also been estimated by the proposed model relatively close to the conventional estimations, since nearly small relative errors are obtained using the ANN-based model compared to the conventional analysis techniques, as illustrated in Table 15. This also indicates the reliability of the proposed approach in estimating the model-related variables from the real pressure transient test data for the two cases considered in this article, when the underlying reservoir model has been properly identified by the presented model. Such an accuracy could not be achieved in estimating the well-testing variables unless the model is trained with a sufficiently large and comprehensive training data set covering wide ranges of the most influencing parameters. Dealing with large numbers of parameters to generate an extensive training data set in a manageable time and effort (by conducting a fewer number of experiments) has been effectively achieved using the DOE technique in this article.

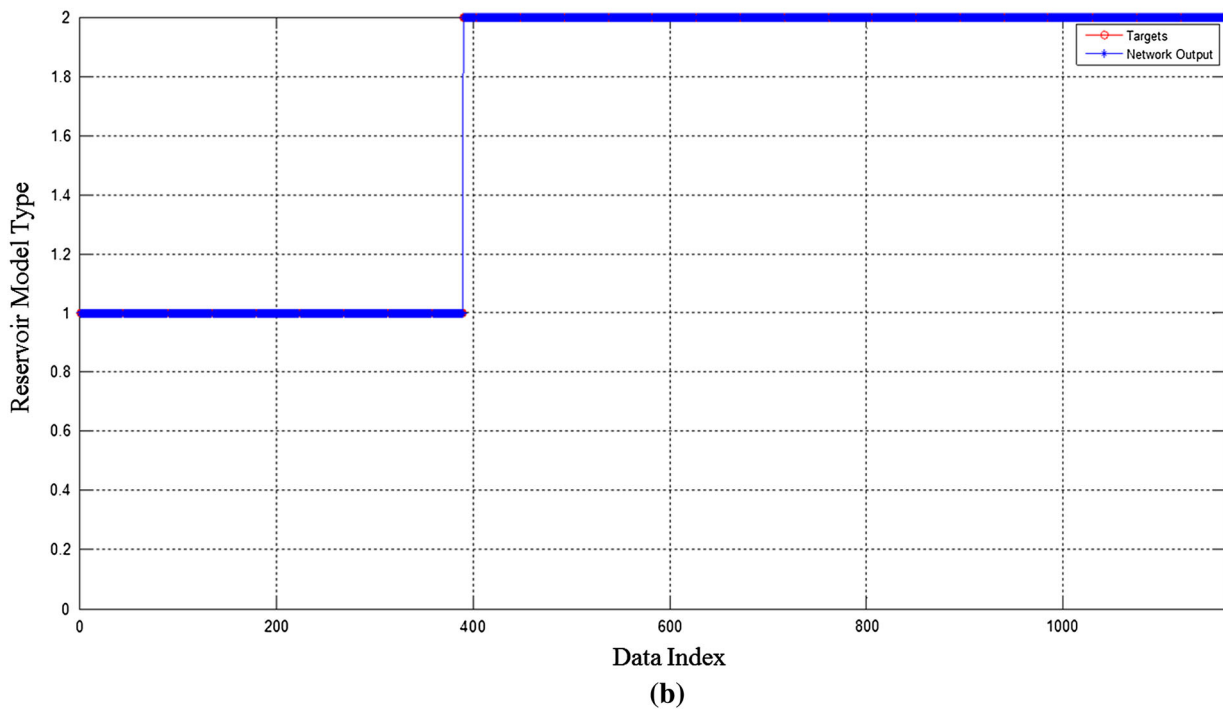
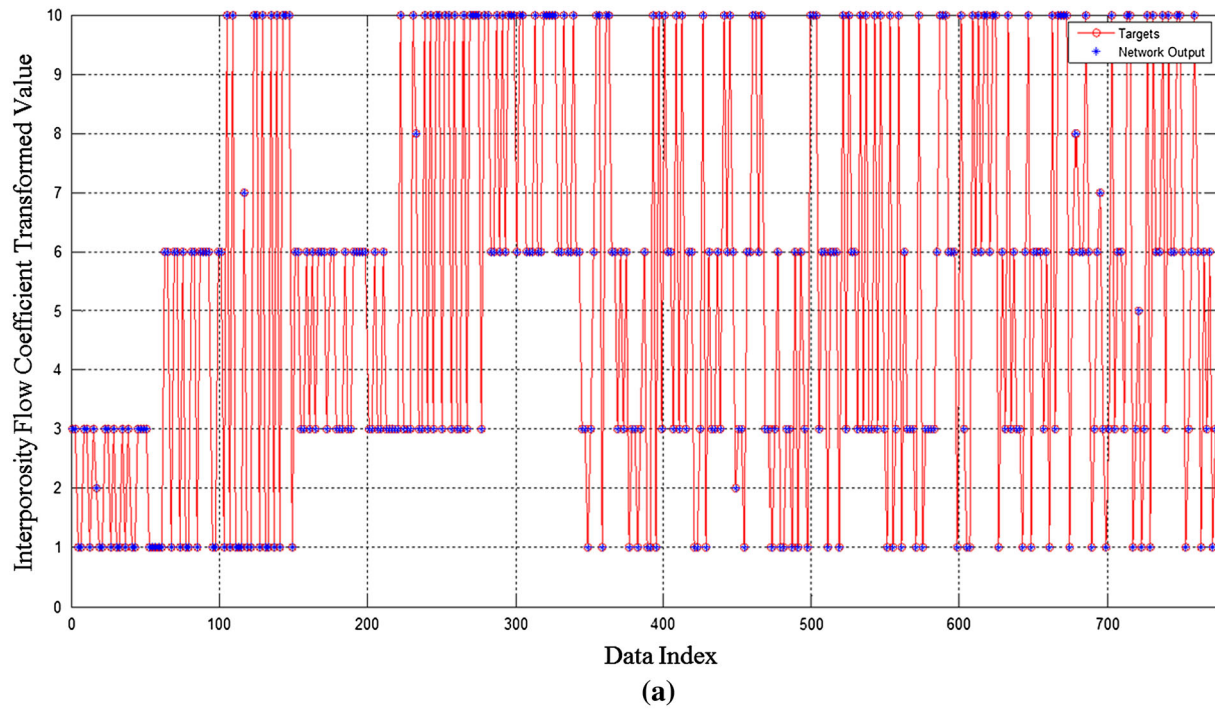


**Fig. 13** Plots of targets versus PNN outputs of **a** inter-porosity flow coefficient transformed values, and **b** type of reservoir model. The numbers 1 and 2 on the y-axis of the plot (b) correspond to the VH and VDP models, respectively

**Conclusions**

1. A new methodology based on ANNs is proposed in this article to automate the process of well-testing interpretation and analysis. The presented approach enables conceptual reservoir model identification and

estimation of model-related parameters from the pressure derivative plots using different types of ANNs.  
 2. Experimental design is executed to select the most influential variables affecting the well-testing designs. The fractional factorial design is also implemented to

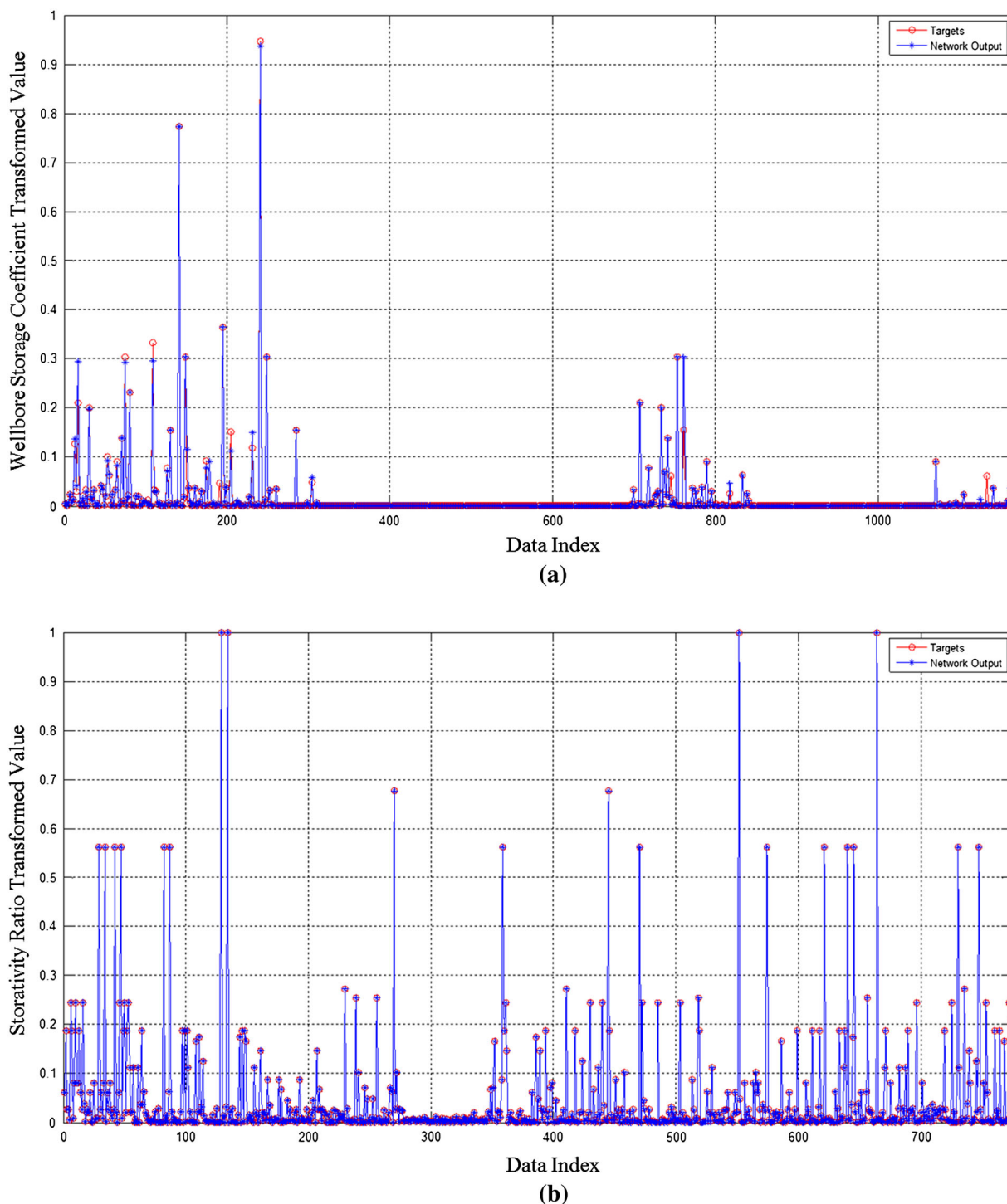


**Fig. 14** Plots of targets versus GRNN outputs of **a** wellbore storage coefficient transformed values, and **b** storativity ratio transformed values

3. The pressure derivative plots are primarily sampled at a limited number of data points, undergone by dimensionality reduction techniques, and finally normalized prior to introduction to the neural network models.

4. Two different reservoir models including homogeneous and double-porosity systems are investigated in this article; so the model-related parameters that will be estimated using the proposed model include permeability, skin factor and dimensionless wellbore storage coefficient (for all kinds of reservoir models)

**Table 13** Performance of the proposed neural network models for estimating the well-testing model parameters and identifying the conceptual reservoir model

Variable	Permeability	Skin factor	Storativity ratio	Wellbore storage coefficient	Reservoir model	Inter-porosity flow coefficient
Data mining task	Estimation				Classification	
Type of neural network	MLP		GRNN		PNN	
Network performance criterion	MSE				Misclassification rate	
Network performance value	$1.35 \times 10^{-4}$	$2.94 \times 10^{-5}$	$5.33 \times 10^{-5}$	$6.74 \times 10^{-5}$	0	0

**Table 14** Estimation of model-related parameters and the well-testing model diagnosis using the conventional analysis techniques and the proposed ANN-based approach (The numbers in parentheses, where provided, are the corresponding values in SI units)

Method of analysis	Test number	Model type	$K$ , md (m <sup>2</sup> )	$S$	$C_D$	$\omega$	$\lambda$
Conventional approach	1	VDP	0.26 (2.57E–16)	–3.3	3	0.71	1.0E–08
	2		17.25 (1.70E–14)	5.52	101	0.232	1.1E–08
	3		131 (1.29E–13)	–7.6	22,800	0.58	1.0E–4
	4	VH	5.8 (5.72E–15)	–5.5	135	–	–
	5		98.5 (9.76E–14)	–6.1	310	–	–
	6		130 (1.28E–13)	14.05	50	–	–
	7		455 (4.49E–13)	17.2	58.5	–	–
Proposed Approach	1	VDP	0.24 (2.37E–16)	–3.09	2.9	0.74	1.0E–08
	2		16.62 (1.64E–14)	5.6	96.92	0.226	1.0E–08
	3		136.87 (1.35E–13)	–7.5	22,448	0.633	1.0E–04
	4	VH	5.38 (5.31E–15)	–5.98	137.74	–	–
	5		100.72 (9.94E–14)	–6.14	314.78	–	–
	6		121.05 (1.19E–13)	15.05	48.06	–	–
	7		422.05 (4.17E–13)	18.4	57	–	–

**Table 15** Relative errors of estimations (in percentage) using the proposed ANN-based model in comparison with the conventional analysis results

Test number	$K$	$S$	$C_D$	$\omega$	$\lambda$
1	7.69	6.36	3.33	4.23	0.00
2	3.65	1.45	4.04	2.59	9.09
3	4.48	1.32	1.54	9.14	0.00
4	7.24	8.73	2.03	–	–
5	2.25	0.66	1.54	–	–
6	6.88	7.12	3.88	–	–
7	7.24	6.98	2.56	–	–
Average of All tests	5.64	4.66	2.70	5.32	3.03

and storativity ratio and inter-porosity flow coefficient (in the case of double-porosity systems).

- Two MLP networks are designed in this study to estimate the permeability and skin factor in their

output neurons. The dimensionless wellbore storage coefficient and storativity ratio are estimated using two different GRNNs, while two different PNNs are employed to predict the value of inter-porosity flow



coefficient and classify the well-testing interpretation model.

6. To involve some other well-testing variables in the estimation process, the transformed values of the model-related parameters are used as the targets for training the neural network models. To estimate the model-related parameters for a given pressure derivative plot using the trained neural networks, the network outputs are converted back to the expected variables using the proper equations.
7. The validation results using the real field buildup test data confirm that the proposed models generate reliable results both in the case of identifying the correct reservoir models and estimating the model-related parameters using the pressure derivative plots compared to the results of conventional well-testing analysis techniques.
8. Unlike the conventional analysis techniques in which the well-testing reservoir models are determined from the visual inspection of the pressure derivative plots, ANNs are trained with the representative examples to recognize the underlying reservoir model and estimate the model-related properties. So ANN-based models are very helpful especially when dealing with the complex patterns on the pressure derivative curves. The great advantages of the ANN-based approach relates to the improvements in the pattern recognition problem compared to the conventional techniques.

## Future works

1. The well-testing interpretation and analysis model presented in this article employs only the pressure derivative plots as inputs to the model. Using the same approach to identify the conceptual reservoir model and to estimate the model-related parameters from other diagnostic plots such as semi-log or linear graphs is recommended for future works.
2. The current research shows the capabilities of the proposed ANN-based approach for the well-testing analysis of the homogeneous and double-porosity systems. Although the proposed approach is investigated by these two types of reservoir models in this article, it is not exclusive to any specific model and could be applied to any system with any types of fluid, well geometry and reservoir structure, provided that the proposed model is re-trained using the proper examples generated for the set of those models. Using other conceptual reservoir models and considering more complex hydrocarbon

systems or fluids like gas condensate reservoirs and horizontal/deviated wells are, therefore, highly encouraged.

**Open Access** This article is distributed under the terms of the Creative Commons Attribution 4.0 International License (<http://creativecommons.org/licenses/by/4.0/>), which permits unrestricted use, distribution, and reproduction in any medium, provided you give appropriate credit to the original author(s) and the source, provide a link to the Creative Commons license, and indicate if changes were made.

## References

- Alajmi M, Ertekin T (2007) The development of an artificial neural network as a pressure transient analysis tool for applications in double-porosity reservoirs. Paper SPE 108604 presented at the SPE Asia Pacific oil and gas conference and exhibition, Jakarta, Indonesia
- Al-Kaabi AU, Lee WJ (1990) An artificial neural network approach to identify the well test interpretation model: applications. Paper SPE 20552 presented at the 65th annual technical conference and exhibition, New Orleans, LA
- Al-Kaabi AU, Lee WJ (1993) Using artificial neural networks to identify the well test interpretation model. Paper SPE 20332 presented at the SPE petroleum computer conference, Denver
- Allain OF, Horne RN (1990) Use of artificial intelligence in well-test interpretation. JPT 42(3):342–349. doi:[10.2118/18160-PA](https://doi.org/10.2118/18160-PA)
- Antony J (2003) Design of experiments for engineers and scientists. Butterworth-Heinemann, Oxford
- Athichanagorn S, Horne RN (1995) Automatic parameter estimation from well test data using artificial neural network. Paper SPE 30556 presented at the SPE annual technical conference and exhibition, Dallas, USA
- Aydinoglu G, Bhat M, Ertekin T (2002) Characterization of partially sealing faults from pressure transient data: an artificial neural network approach. Paper SPE 78715 presented at the SPE eastern regional meeting, Lexington, Kentucky, USA
- Bourdarot G (1999) Well testing: interpretation methods. Editions TECHNIP
- Bowden GJ, Dandy GC, Maier HR (2005) Input determination for neural network models in water resources applications: part 1—background and methodology. J Hydrol 301(1–4):75–92
- Cybenko G (1989) Approximation by superpositions of a sigmoidal function. Math Control Signal 2(4):303–314
- Deng Y, Chen Q, Wang J (2000) The artificial neural network method of well-test interpretation model identification and parameter estimation. Paper SPE 64652 presented at the SPE international oil and gas conference and exhibition, Beijing, China
- Ershaghi I, Li X, Hassibi M, Shikari Y (1993) A robust neural network model for pattern recognition of pressure transient test data. Paper SPE 26427 presented at the SPE annual technical conference and exhibition, Houston, Texas
- Gibbs MS, Morgan N, Maier HR, Dandy GC, Nixon J, Holmes M (2006) Investigation into the relationship between chlorine decay and water distribution parameters using data driven methods. Math Comput Model 44(5):485–498
- Haykin S (1999) Neural networks, a comprehensive foundation. Prentice Hall, Upper Saddle River
- Hinkelmann K, Kempthorne O (2007) Design and analysis of experiments. Introduction to experimental design, vol 1. Wiley, New York

- Jamshidnezhad M (2015) Experimental design in petroleum reservoir studies. Gulf Professional Publishing, Elsevier, Oxford. doi:[10.1016/B978-0-12-803070-7.00001-6](https://doi.org/10.1016/B978-0-12-803070-7.00001-6)
- Jeirani Z, Mohebbi A (2006) Estimating the initial pressure, permeability and skin factor of oil reservoirs using artificial neural networks. *J Petrol Sci Eng* 50:11–20
- Juniardi IR, Ershaghi I (1993) Complexities of using neural network in well test analysis of faulted reservoirs. Paper SPE 26106 presented at the western regional meeting, Anchorage, Alaska
- Kharrat R, Razavi SM (2008) Determination of reservoir model from well test data using an artificial neural network. *Sci Iran* 15(4):487–493
- Kumoluyi AO, Daltaban TS, Archer JS (1995) Identification of well-test models by use of higher-order neural networks. Paper SPE 27558 presented at the SPE european petroleum computer conference, Aberdeen
- Lee WJ (1982) Well testing. Society of petroleum engineers of AIME
- Li X, Zecchin AC, Maier HR (2014) Selection of smoothing parameter estimators for general regression neural networks—applications to hydrological and water resources modelling. *Environ Modell Softw* 59:162–186. doi:[10.1016/j.envsoft.2014.05.010](https://doi.org/10.1016/j.envsoft.2014.05.010)
- Montgomery DC (2002) Design and analysis of experiments. Wiley, New York
- Nelson PR (1983) A comparison of sample sizes for the analysis of means and the analysis of variance. *J Qual Technol* 15:33–39
- Rosenblatt FX (1961) Principles of neurodynamics: perceptrons and the theory of brain mechanisms. Spartan Books, Washington
- Rumelhart DE, Geoffrey EH, Williams RJ (1986) Learning internal representations by error propagation. In: Rumelhart DE, McClelland JL, PDP research group (eds) *Parallel distributed processing: explorations in the microstructure of cognition*. Foundations, vol 1. MIT Press, Cambridge
- Specht DF (1991) A general regression neural network. *Neural Netw IEEE Trans* 2(6):568–576
- Specht DF (1990) Probabilistic neural networks. *Neural Netw* 3:109–118. doi:[10.1016/0893-6080\(90\)90049-Q](https://doi.org/10.1016/0893-6080(90)90049-Q)
- Sung W, Yoo I, Ra S, Park H (1996) Development of the HT-BP neural network system for the identification of a well-test interpretation model. Paper SPE 30974 presented at the SPE eastern regional meeting, Morgantown
- Vaferi B, Eslamloueyan R, Ayatollahi S (2011) Automatic recognition of oil reservoir models from well testing data by using multi-layer perceptron networks. *J Petrol Sci Eng* 77:254–262

## Web References

- Ben-Hur A, Weston J (2015) A user's guide to support vector machines. Technical report. <http://pyml.sourceforge.net/doc/howto.pdf>. Accessed 10 Feb 2016
- French A, Macedo M, Poulsen J, Waterson T, Yu A (2015) Multivariate analysis of variance (MANOVA). <http://userwww.sfsu.edu/~efc/classes/biol710/manova/MANOVAnewest.pdf>. Accessed 10 Feb 2016
- Ientilucci EJ (2003) using the singular value decomposition. <http://www.cis.rit.edu/~ejipci/research.htm>. Accessed 10 Feb 2016
- IHS Energy Inc (2015) Well testing and rate transient analysis consulting. <http://cdn.ihs.com/www/images/Fekete-WellTest-Fundamentals.png>. Accessed 10 Feb 2016
- NIST Information Technology Laboratory (2012) NIST/SEMATECH e-handbook of statistical methods. [www.itl.nist.gov/div898/handbook/pri/section3/pri335.htm](http://www.itl.nist.gov/div898/handbook/pri/section3/pri335.htm). Accessed 10 Feb 2016
- Sundararajan K (2015) Design of experiments—a primer. <http://www.isixsigma.com/tools-templates/design-of-experiments-doe/design-experiments-%E2%90%93-primer/>. Accessed 10 Feb 2016